

# CrystEngComm

Accepted Manuscript



This is an *Accepted Manuscript*, which has been through the Royal Society of Chemistry peer review process and has been accepted for publication.

*Accepted Manuscripts* are published online shortly after acceptance, before technical editing, formatting and proof reading. Using this free service, authors can make their results available to the community, in citable form, before we publish the edited article. We will replace this *Accepted Manuscript* with the edited and formatted *Advance Article* as soon as it is available.

You can find more information about *Accepted Manuscripts* in the [Information for Authors](#).

Please note that technical editing may introduce minor changes to the text and/or graphics, which may alter content. The journal's standard [Terms & Conditions](#) and the [Ethical guidelines](#) still apply. In no event shall the Royal Society of Chemistry be held responsible for any errors or omissions in this *Accepted Manuscript* or any consequences arising from the use of any information it contains.

## ARTICLE

# The first photochromic bimetallic assemblies based on Mn(III) and Mn(II) Schiff-base (salpn, dapsc) complexes and pentacyanonitrosylferrate†

Cite this: DOI: 10.1039/x0xx00000x

Received 00th February 2015,  
Accepted 00th 2015

DOI: 10.1039/x0xx00000x

www.rsc.org/

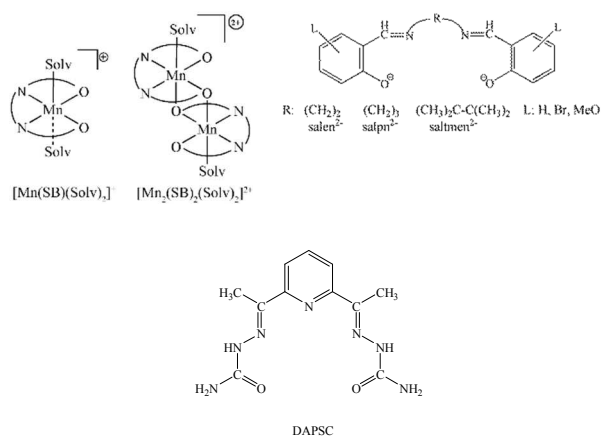
Vyacheslav A. Kopotkov,<sup>a\*</sup> Valentina D. Sasnovskaya,<sup>a</sup> Denis V. Korchagin,<sup>a</sup> Roman B. Morgunov,<sup>a</sup> Sergey M. Aldoshin,<sup>a</sup> Sergey V. Simonov,<sup>b</sup> Leokadiya V. Zorina,<sup>b\*</sup> Dominik Schaniel,<sup>c,d</sup> Theo Woike,<sup>e\*</sup> and Eduard B. Yagubskii<sup>a\*</sup>

Four cyano-bridged bimetallic complexes, {[Mn(salpn)]<sub>2</sub>[Fe(CN)<sub>5</sub>NO]}<sub>n</sub> (**1**), {[Mn(salpn)(CH<sub>3</sub>OH)]<sub>4</sub>[Mn(CN)<sub>5</sub>NO]}[C(CN)<sub>3</sub>]·3H<sub>2</sub>O (**2**), {[Mn(dapsc)][Fe(CN)<sub>5</sub>NO]·0.5CH<sub>3</sub>OH·0.25H<sub>2</sub>O]}<sub>n</sub> (**3**) and {[Mn(salpn)(CH<sub>3</sub>OH)]<sub>4</sub>[Fe(CN)<sub>5</sub>NO]}(ClO<sub>4</sub>)<sub>2</sub>·4H<sub>2</sub>O (**4**), where salpn<sup>2-</sup> = *N,N'*-1,3-propylenebis(salicylideneiminato) dianion, dapsc = 2,6-diacetylpyridine bis(semicarbazone), have been synthesized and structurally characterized by single crystal X-ray diffraction. In **1**, the nitroprusside anion [Fe(CN)<sub>5</sub>NO]<sup>2-</sup> coordinates with four [Mn(salpn)]<sup>+</sup> via four co-planar CN<sup>-</sup> groups, whereas each [Mn(salpn)]<sup>+</sup> links two [Fe(CN)<sub>5</sub>NO]<sup>2-</sup> ions, which results in a two-dimensional network. The structure of **3** contains two independent neutral infinite chains {[Mn(dapsc)][Fe(CN)<sub>5</sub>(NO)]}<sub>∞</sub> consisting of alternating cationic [Mn<sup>II</sup>(dapsc)]<sup>2+</sup> and anionic [Fe<sup>II</sup>(CN)<sub>5</sub>(NO)]<sup>2-</sup> units connected through cyanide bridges. The cation complexes **2** and **4** have the pentanuclear molecular structure in which four [Mn(salpn)(MeOH)]<sup>+</sup> fragments are linked by the [Mn(CN)<sub>5</sub>NO]<sup>3-</sup> or [Fe(CN)<sub>5</sub>(NO)]<sup>2-</sup> moieties, respectively. The magnetic and photochromic properties of **1**, **3** have been studied. The thermal magnetic behaviour of the complexes indicates the presence of weak antiferromagnetic interactions between Mn<sup>3+</sup> or Mn<sup>2+</sup> mediated by diamagnetic [Fe(CN)<sub>5</sub>NO]<sup>2-</sup> bridges. Irradiation of **1**, **3** with light gives birth to the long-lived metastable states of nitroprusside.

## Introduction

Manganese(III) ions form mono- or dimeric high-spin complexes with the tetradentate (N<sub>2</sub>O<sub>2</sub>) Schiff bases (SB) of salen type (salen = *N,N'*-ethylenebis(salicylideneiminato) dianion), Scheme 1.<sup>1</sup> These complexes are extensively used as building blocks for the development of magnetic materials with variable dimensionality through the replacement of the neutral terminal ligands for paramagnetic bridging groups, namely, the hexacyanometalate anions ([M(CN)<sub>6</sub>]<sup>3-</sup>, M = Fe, Cr, Mn, Ru, Os).<sup>2</sup> Self-assemblies of [Mn(SB)]<sup>+</sup> and the hexacyanometalates bring a rich variety of structures (0D clusters, 1D chains, 2D and 3D networks) showing the ferromagnetic superexchange coupling. Molecular nanomagnets such as single-molecule magnets (SMMs)<sup>2b-d,3</sup> or single-chain magnets (SCMs)<sup>2h,4</sup> exhibiting a slow relaxation of magnetization have been found among them. Different from the hexacyanometalates which were widely used in combination with [Mn(SB)]<sup>+</sup>, only few examples were known with other cyanide-bridged building blocks, in particular with the paramagnetic [Cr<sup>I+</sup>(CN)<sub>5</sub>NO]<sup>3-5</sup>

and the diamagnetic nitroprusside (NP) [Fe<sup>2+</sup>(CN)<sub>5</sub>NO]<sup>2- 6</sup> anions. The interest in the nitroprusside anion is connected with its photochromic properties.<sup>7</sup> Irradiation of Na<sub>2</sub>NP with light at a wavelength of 380– 580 nm generates two long-lived metastable states (MS1 and MS2), which can persist for several months at a temperature below 150 K. The reverse transition from the metastable states to the ground state (GS) occurs when Na<sub>2</sub>NP is illuminated at a wavelength of 600– 900 nm or heated above the decay temperature of the metastable states, ~ 150 K. Upon irradiation with near-IR light at 900– 1200 nm, MS1 is partially converted into MS2. The existence of long-lived metastable states in sodium nitroprusside is due to the metal to ligand charge transfer from Fe<sup>2+</sup> to the NO group accompanied by isomerization of the NO group. The NO group is bound to iron through the nitrogen atom in the ground state and through the oxygen atom in MS1.<sup>7b,c</sup> In MS2, the iron atom is coordinated to both atoms of the nitrosyl group.<sup>7d,e</sup> To isomerize the NO group under exposure to light, some free space in the structure is necessary.<sup>7a-c</sup>



Scheme 1

The use of photochromic blocks in combination with magnetic blocks is one of the synthetic approaches to develop photomagnetic materials.<sup>6a,b,8</sup> However, the known bimetallic assemblies containing Mn(SB) cations (SB = salen, 3-MeOsalen, 5-Brsalen, 5-Brsalpn, saltmen, Scheme 1) and  $[\text{Fe}(\text{CN})_5\text{NO}]^{2-}$  anion did not show photoactivity.<sup>6a,b</sup> The loss of photochromism related to the nitroprusside anion is probably connected with a disorder in arrangement of the nitrosyl group in crystalline lattice and/or the steric effects. So, the NO group is disordered between two positions in the complex with  $[\text{Mn}(3\text{-MeOsalen})]$  and is well enclosed in the “cages” formed by the ligands salen, 5-Brsalen, 5-Brsalpn and saltmen.<sup>6a,b</sup> It should also be noted that the polynuclear heterometallic compounds  $\{[\text{Mn}_4(\text{hmp})_6(\text{NO}_3)_2 \text{Fe}(\text{CN})_5\text{NO}] \cdot 4\text{CH}_3\text{CN}\}_n$  and  $[\text{Mn}(\text{acacen})\text{H}_2\text{O}]_2[\text{Fe}(\text{CN})_5\text{NO}] \cdot \text{C}_2\text{H}_5\text{OH}$ , in the structures of which the magnetic  $[\text{Mn}^{\text{II}}\text{Mn}^{\text{III}}_2(\text{hmp})_6]$  or  $[\text{Mn}^{\text{III}}(\text{acacen})\text{H}_2\text{O}]$  units are linked via CN groups of nitroprusside anions, do not possess photochromism.<sup>9</sup> In these assemblies, the NO group is disordered and is clamped between hmp ligands.<sup>9a</sup> It is also speculated that the photoinduced metastable states are not generated when the cyanido groups of nitroprusside anion are coordinating with  $\text{Mn}^{\text{III}}$  metal ions.<sup>6a,b,9b</sup>

In contrast to<sup>6b</sup>, we used here the unsubstituted salpn as SB ligand and another synthetic approach based on the use of the neutral starting complex  $[\text{Mn}(\text{salpn})\text{C}(\text{CN})_3(\text{H}_2\text{O})]$  in combination with  $[\text{Fe}(\text{CN})_5\text{NO}]^{2-}$ . As a result, the new bimetallic material  $\{[\text{Mn}(\text{salpn})]_2[\text{Fe}(\text{CN})_5\text{NO}]\}_n$  (**1**) has been obtained. Its synthesis, structure, magnetic and photochromic properties are presented in the current work. The complex of  $[\text{Mn}(\text{salpn})]$  with pentacyanonitrosylmanganate  $[\text{Mn}^{\text{I}}(\text{CN})_5\text{NO}]^{3-}$ , which is a diamagnetic analog of  $[\text{Cr}^{\text{I}}(\text{CN})_5\text{NO}]^{3-}$  and isoelectronic to  $[\text{Fe}(\text{CN})_5\text{NO}]^{2-}$ , was also synthesized:  $\{[\text{Mn}(\text{salpn})(\text{CH}_3\text{OH})]_4[\text{Mn}(\text{CN})_5\text{NO}]\}^+[\text{C}(\text{CN})_3]^- \cdot 3\text{H}_2\text{O}$  (**2**). Its crystal structure is analyzed.

Another part of the present work deals with the synthesis, structure, magnetic and photochromic properties of the first bimetallic chain complex derived from paramagnetic  $[\text{Mn}^{2+}(\text{dapsc})]^{2+}$  and nitroprusside anion:  $\{[\text{Mn}(\text{dapsc})]$

$[\text{Fe}(\text{CN})_5\text{NO}] \cdot 0.5\text{CH}_3\text{OH} \cdot 0.25\text{H}_2\text{O}\}_n$  (**3**), where dapsc = 2,6-diacetylpyridine bis(semicarbazone), Scheme 1. The complexes of transition metals based on dapsc-ligand reveal the rare occurrence of pentagonal-bipyramidal stereochemistry about a central metal atom, which results from pentacoordination of the nearly planar ligand DAPSC ( $\text{N}_3\text{O}_2$ ), and two axial ligands ( $\text{H}_2\text{O}$  and/or Cl) perpendicular to the equatorial, pentagon plane.<sup>10</sup> These compounds are of considerable interest as new paramagnetic building blocks to form bimetallic assemblies with cyanometallate anions of different type. The axiality of the pentagonal-bipyramidal geometry may lead to strong Ising-type anisotropy.<sup>11</sup> Along with the high-spin ground state, this is responsible for SMM behaviour.

## Experimental

### Materials and General Procedures

All chemicals and solvents used in the synthesis were reagent grade and were used without further purification. The precursors:  $[\text{Mn}_2(\text{salpn})_2(\text{H}_2\text{O})_2](\text{ClO}_4)_2$ , dapsc ligand,  $[\text{Mn}^{\text{II}}(\text{dapsc})\text{Cl}_2] \cdot \text{H}_2\text{O}$ ,  $[\text{Mn}^{\text{III}}(\text{salpn})\text{C}(\text{CN})_3(\text{H}_2\text{O})]$  and  $\text{K}_3[\text{Mn}(\text{CN})_5\text{NO}] \cdot 2\text{H}_2\text{O}$  were prepared according to the literature procedures.<sup>1g,10d,j,12,13</sup> The C, H and N elemental analyses were carried out with a vario MICRO cube analyzing device. The thermogravimetric analysis was performed in argon atmosphere with a heating rate  $5.0 \text{ }^\circ\text{C min}^{-1}$  using a NETZSCH STA 409 C Luxx thermal analyzer, interfaced to a QMS 403 Aelos mass spectrometer, which allows simultaneous thermogravimetry (TG), differential scanning calorimetry (DSC) and mass-spectrometry measurements. Variable-temperature magnetic susceptibility measurement of **1** and **3** was performed with a Quantum Design MPMS SQUID magnetometer. The experimental data were corrected for the sample holder and for the diamagnetic contribution calculated from Pascal constants. The effective magnetic moment was calculated using the equation  $\mu_{\text{eff}} = 2.828 (\chi_{\text{M}} \times T)^{1/2}$ . The infrared spectra were collected with a Thermo-Nicolet 5700 FT-IR spectrometer using a resolution of  $2 \text{ cm}^{-1}$ . Powdered samples were mixed with KBr and pressed to pellets. The KBr pellet was mounted on a copper cold finger using a silver paste for good thermal contact. The sample was cooled down in a vacuum of  $10^{-6}$  mbar to 10 K in an Oxford closed cycle cryostat equipped with KBr windows and a MercuriTC temperature controller. KBr windows allowed the irradiation of the sample with laser light in the visible and near infrared spectral range and IR-absorption measurements down to  $380 \text{ cm}^{-1}$ . Irradiation was carried out with a set of diode-lasers between 405 – 1310 nm using a power of 30 mW resulting in an intensity of  $38 \text{ mW/cm}^2$ . The beam was expanded for homogeneous irradiation of the sample.

### Synthesis

$\{[\text{Mn}(\text{salpn})]_2[\text{Fe}(\text{CN})_5(\text{NO})]\}_n$  (**1**). A solution of  $\text{Na}_2[\text{Fe}(\text{CN})_5\text{NO}] \cdot 2\text{H}_2\text{O}$  (22.18 mg, 0.085 mmol) in 5 mL of

water was added to a solution of  $[\text{Mn}(\text{salpn})\text{C}(\text{CN})_3(\text{H}_2\text{O})]$  (75 mg, 0.169 mmol) in 10 mL of methanol. The mixture was heated to 50 °C. After stirring for 30 min, the resulting dark brown solution was filtered. The filtrate was left undisturbed at room temperature for three days to produce dark brown single crystals suitable for X-ray analysis. The crystals were collected by suction filtration, washed with water, and air-dried. For **1**: yield: 43 mg, 57% Anal. calc. for  $\text{C}_{39}\text{H}_{32}\text{FeMn}_2\text{N}_{10}\text{O}_5$  (886.48): C, 52.82; H, 3.61; N, 15.8%. Found: C, 52.64; H, 3.94; N, 15.33%.

Thermal analysis showed that **1** is stable up to ~ 230 °C (Fig. S1, ESI†). The DSC curve gives an exothermal peak at 251.3 °C, which is associated with the decomposition of complex. As this takes place, in the mass spectrum of the gas phase (Fig. S1, ESI†) the peaks are observed at  $m/z$  17, 18, 26 and 30 corresponding to OH,  $\text{H}_2\text{O}$ , CN and NO groups. The decomposition temperature (251.3 °C) for **1** is close to that (245.7 °C) for the complex  $\{[\text{Mn}(\text{salen})_2[\text{Fe}(\text{CN})_5(\text{NO})]\cdot 2\text{H}_2\text{O}\}_n$  which has a similar crystal structure.<sup>6d</sup>

#### $\{[\text{Mn}(\text{salpn})(\text{CH}_3\text{OH})]_4[\text{Mn}(\text{CN})_5\text{NO}]\}[\text{C}(\text{CN})_3]\cdot 3\text{H}_2\text{O}$

(2). A solution of  $\text{K}_3[\text{Mn}(\text{CN})_5\text{NO}]\cdot 2\text{H}_2\text{O}$  (11.21 mg, 0.03 mmol) in 5 mL of water was added to a solution of  $[\text{Mn}(\text{salpn})\text{C}(\text{CN})_3(\text{H}_2\text{O})]$  (54 mg, 0.121 mmol) in 10 mL of methanol. The mixture was heated to 60 °C. After stirring for 30 min, the resulting dark brown solution was filtered. The filtrate was left undisturbed at room temperature for 3– 5 days to produce dark brown single crystals. The crystals for X-ray analysis were kept in contact with the mother liquid. The composition of the crystals,  $\{[\text{Mn}(\text{salpn})(\text{CH}_3\text{OH})]_4[\text{Mn}(\text{CN})_5\text{NO}]\}[\text{C}(\text{CN})_3]\cdot 3\text{H}_2\text{O}$ , has been established from the X-ray analysis. IR:  $\nu_{(\text{NO})} = 1751.0$ ,  $\nu_{(\text{C}\equiv\text{N})} = 2100.9$ , 2174.0,  $\nu_{(\text{C}=\text{N})} = 1615.0$   $\text{cm}^{-1}$ . The band of the NO stretching vibration in the IR spectrum of **2** is shifted to higher wavenumbers in comparison to the starting material  $\text{K}_3[\text{Mn}(\text{CN})_5\text{NO}]\cdot 2\text{H}_2\text{O}$  (1725  $\text{cm}^{-1}$ ).<sup>13</sup>

#### $\{[\text{Mn}(\text{dapsc})][\text{Fe}(\text{CN})_5\text{NO}]\cdot 0.5\text{CH}_3\text{OH}\cdot 0.25\text{H}_2\text{O}\}_n$

(3). The crystals of **3** have been obtained by slow diffusion within a week of the starting reagents,  $\text{Na}_2[\text{Fe}(\text{CN})_5\text{NO}]\cdot 2\text{H}_2\text{O}$  (49 mg, 0.16 mmol) in 3 mL of water and  $[\text{Mn}^{\text{II}}(\text{dapsc})\text{Cl}_2]\cdot \text{H}_2\text{O}$  (70 mg, 0.16 mmol) in 20 mL methanol, into  $\text{CH}_3\text{OH}$ . The resulting crystals were collected by filtration, washed with water and methanol and dried in a vacuum. For **3**: yield: 50 mg, 54%. Anal. calc. for  $\text{C}_{16}\text{H}_{15}\text{FeMnN}_3\text{O}_3$  (568.725): C, 35.05; H, 2.75; N, 33.21%. Found: C, 35.15; H, 3.02; N, 33.22%. The elemental analysis indicates a loss of lattice solvents ( $\text{H}_2\text{O}$  and  $\text{CH}_3\text{OH}$ ) upon drying relative to the crystallographically characterized species. The crystals for X-ray analysis were kept in contact with the mother liquid.

The thermogram of freshly prepared crystals **3**, which were dried in air before the TG-DSC measurements, demonstrates the mass loss of 2.84% in the temperature range 70-200 °C, which corresponds to the loss 0.5 molecule of lattice solvents  $\text{CH}_3\text{OH}$  (calcd. 2.81%), Fig. S2, ESI†. In the mass spectrum recorded in the gas phase, the peaks are observed at  $m/z$  15, 30 and 31 corresponding to the fragments of methanol molecule ( $\text{CH}_3$ :  $m/z$

= 15;  $\text{CH}_2\text{O}$ :  $m/z$  = 30;  $\text{CH}_3\text{O}$ :  $m/z$  = 31). The second weight-loss step appears at temperature below 250 °C with an exothermic peak at 286.6 °C, which corresponds to the decomposition of complex. As this takes, ions with  $m/z$  17, 26, 30 (OH, CN, NO) are observed in the mass spectrum. Unlike the freshly prepared sample of complex **3**, after drying under vacuum, the complex shows no weight loss up to 200 °C.

#### $\{[\text{Mn}(\text{salpn})(\text{CH}_3\text{OH})]_4[\text{Fe}(\text{CN})_5\text{NO}]\}(\text{ClO}_4)_2\cdot 4\text{H}_2\text{O}$

(4). A solution of  $\text{Na}_2[\text{Fe}(\text{CN})_5\text{NO}]\cdot 2\text{H}_2\text{O}$  (10.67 mg, 0.036 mmol) in 5 mL of water was added to a solution of  $[\text{Mn}_2(\text{salpn})_2(\text{H}_2\text{O})_2](\text{ClO}_4)_2$  (65 mg, 0.072 mmol) in 12 mL of methanol. The mixture was heated to 60 °C. After stirring for 30 min, the resulting dark brown solution was filtered. The filtrate was left undisturbed at room temperature for 3-5 days to produce dark single crystals. The crystals for X-ray analysis were kept in contact with the mother liquid. The composition of the crystals,  $\{[\text{Mn}(\text{salpn})(\text{CH}_3\text{OH})]_4[\text{Fe}(\text{CN})_5\text{NO}]\}(\text{ClO}_4)_2\cdot 4\text{H}_2\text{O}$ , has been established from the X-ray analysis. IR:  $\nu_{(\text{NO})} = 1904.0$ ,  $\nu_{(\text{C}\equiv\text{N})} = 2150.7$ ,  $\nu_{(\text{C}=\text{N})} = 1613.0$ ,  $\nu_{(\text{C}-\text{O})} = 1068.4$   $\text{cm}^{-1}$ .

It should be noted that the synthesis of complexes **2** and **4** affords the mixture of products. The powder X-ray diffraction of the bulk samples of **2** and **4** showed that these samples are not single-phase ones. Moreover, the data of elemental analysis for **2** and **4** are not in a good agreement with their composition determined from the single crystal X-ray analysis.

**X-ray Crystallography.** Single crystal X-ray diffraction experiments were carried out on CCD diffractometers Agilent Xcalibur with EOS detector for crystals **1** and **2** and Oxford Diffraction Gemini-R with Ruby detector for crystal **3**. The data sets were collected at 150.0(1) K for **1**, **2** and 140(1) K for **3** using  $\text{MoK}\alpha$  ( $\lambda = 0.71073\text{\AA}$ ) radiation and treated by CrysAlisPro software for cell refinement, data collection, and data reduction with empirical absorption correction (Scale3AbsPack) of the experimental intensities.<sup>14</sup> The structures were solved by direct methods. The positions and thermal parameters of non-hydrogen atoms were refined anisotropically by the full-matrix least-squares method. Hydrogen atom positions were localized from the difference map (for **1**) or placed in the idealized positions (for **2** and **3**) and refined isotropically. The crystallographic data for **1-3** are summarized in Table 1. All calculations were performed with the SHELXTL program package<sup>15</sup> for **1**, **2** and the SHELX97 program<sup>16</sup> for **3**.

## Results and discussion

### Synthesis

The polynuclear complexes  $\{[\text{Mn}(\text{salpn})]_2[\text{Fe}(\text{CN})_5\text{NO}]\}_n$  (**1**) and  $\{[\text{Mn}(\text{salpn})(\text{CH}_3\text{OH})]_4[\text{Mn}(\text{CN})_5\text{NO}]\}[\text{C}(\text{CN})_3]\cdot 3\text{H}_2\text{O}$  (**2**) are obtained under similar reaction conditions, which consist in the addition of an aqueous solution of  $\text{Na}_2[\text{Fe}(\text{CN})_5\text{NO}]$  or  $\text{K}_3[\text{Mn}(\text{CN})_5\text{NO}]$  to a methanol solution of the neutral complex  $[\text{Mn}(\text{salpn})\text{C}(\text{CN})_3(\text{H}_2\text{O})]$  synthesized by us recently.<sup>12</sup> Single

crystals have been obtained from the mother liquor on standing at room temperature for several days. Note that the use of the cation complex  $[\text{Mn}_2(\text{salpn})_2(\text{H}_2\text{O})_2](\text{ClO}_4)_2$  instead of neutral  $[\text{Mn}(\text{salpn})\text{C}(\text{CN})_3(\text{H}_2\text{O})]$  in the reaction with nitroprusside by

analogy with the approach described in the literature<sup>6</sup> gives a complex of another composition,  $\{[\text{Mn}(\text{salpn})(\text{CH}_3\text{OH})_4[\text{Fe}(\text{CN})_5\text{NO}]](\text{ClO}_4)_2 \cdot 4\text{H}_2\text{O}$  (**4**), which has been established

**Table 1** Crystal data and structural refinement parameters for the complexes **1-3**

Crystal parameters	<b>1</b>	<b>2</b>	<b>3</b>
Chemical formula	$\text{C}_{39}\text{H}_{32}\text{Fe}_1\text{Mn}_2\text{N}_{10}\text{O}_5$	$\text{C}_{84}\text{H}_{80}\text{Mn}_5\text{N}_{20}\text{O}_{17}$	$\text{C}_{16.5}\text{H}_{17.5}\text{FeMnN}_{13}\text{O}_{3.75}$
Formula weight	886.48	1916.38	568.72
Cell setting	tetragonal	monoclinic	orthorhombic
Space group, Z	$P4/ncc$ , 4	$C2/m$ , 2	$Pna2_1$ , 8
Temperature (K)	150(1)	150(1)	140(1)
<i>a</i> (Å)	14.5312(2)	22.121(2)	26.821(2)
<i>b</i> (Å)	14.5312(2)	17.3201(5)	17.721(2)
<i>c</i> (Å)	18.0950(6)	16.135(2)	10.2330(8)
$\alpha$ (°)	90	90	90
$\beta$ (°)	90	135.24(2)	90
$\gamma$ (°)	90	90	90
<i>V</i> , (Å <sup>3</sup> )	3820.9(2)	4353.3(6)	4863.7(8)
$\rho_{\text{calcd}}$ (g/cm <sup>3</sup> )	1.541	1.462	1.553
$\mu$ , cm <sup>-1</sup>	1.084	0.784	1.166
<i>R</i> <sub>effs</sub> collected/unique	7636 / 1949	8986 / 4584	32385 / 13894
<i>R</i> <sub>int</sub>	0.0259	0.0259	0.0383
$\theta$ range (°)	2.80 to 26.32	2.96 to 26.32	1.90 to 30.00
Parameters refined	166	305	657
Final <i>R</i> <sub>1</sub> , <i>wR</i> <sub>2</sub> [ <i>I</i> > 2 $\sigma$ ( <i>I</i> )]	0.0307 (0.0776)	0.0624 (0.1611)	0.0492 (0.1114)
<i>R</i> <sub>1</sub> ( <i>wR</i> <sub>2</sub> )	0.0375 (0.0824)	0.0787 (0.1703)	0.0533 (0.1141)
GOF (F <sup>2</sup> )	1.085	1.055	1.036
CCDC no.	1022451	1022452	1022887

from the X-ray analysis (Fig. S3, ESI<sup>†</sup>). The pentanuclear  $[\text{Mn}^{\text{III}}_4\text{Fe}^{\text{II}}]^{2-}$  units in **4** are discrete and their structure is similar to that of the  $[\text{Mn}^{\text{III}}_4\text{Mn}^{\text{I}}]^-$  units in **2** (see below). The crystals **4** had a poor quality which did not allow to refine their structure. The complex  $\{[\text{Mn}(\text{dapsc})][\text{Fe}(\text{CN})_5\text{NO}] \cdot 0.5\text{CH}_3\text{OH} \cdot 0.25\text{H}_2\text{O}\}_n$  (**3**) has been synthesized in the reaction of  $[\text{Mn}(\text{dapsc})\text{Cl}_2] \cdot \text{H}_2\text{O}^{10j}$  with  $\text{Na}_2[\text{Fe}(\text{CN})_5\text{NO}]$ . The crystals suitable for X-ray analysis have been obtained by slow diffusion of the starting reagents into a solvent ( $\text{CH}_3\text{OH}$ ).

### Crystal structures

Complex **1** crystallizes in the tetragonal  $P4/ncc$  space group and consists of a 2D neutral network  $\{[\text{Mn}(\text{salpn})_2[\text{Fe}(\text{CN})_5(\text{NO})]]_n\}$ . The crystal structure of **1** is similar to that of  $\{[\text{Mn}(\text{salen})_2[\text{Fe}(\text{CN})_5(\text{NO})]]_n\}$  and  $\{[\text{Mn}(5\text{-Brsalen})_2[\text{Fe}(\text{CN})_5(\text{NO})]]_n\}$  complexes<sup>6a-c</sup>. Fig. 1 shows the basic building unit and its connection mode in complex **1**.

The atom Mn(1) lies on a twofold axis, the asymmetric unit of complex **1** includes only a half of  $[\text{Mn}(\text{salpn})]^+$ . The Mn<sup>III</sup> atom has a distorted octahedral coordination with two N and two O atoms of salpn ligand in the equatorial plane, and two N(4) atoms of cyanide bridge C(11)–N(4) from the  $[\text{Fe}(\text{CN})_5\text{NO}]^{2-}$  anion in axial positions.

The atom Mn<sup>III</sup> has an axially elongated distorted octahedral coordination as a result of the Jahn–Teller effect; the bond distance in the axial position (Mn(1)–N(4) = 2.288 Å) is longer than that in the equatorial plane (the average Mn–X bond length in the equatorial plane is 1.954(2) Å, X = N or O atom of the salpn ligand; Table 2.).

In the  $[\text{Fe}(\text{CN})_5\text{NO}]^{2-}$  fragment, the Fe(1) center, nitrosyl group and axial (ax) cyanide group lie on a fourfold axis. As a result, the Fe(1)–N(3)–O(3) angle is linear and all equatorial (eq) C(11)–N(4) ligands are symmetrically equivalent. The bond lengths Fe(1)–C<sup>ax</sup> and Fe(1)–C<sup>eq</sup> differ inconsiderably and are equal to 1.935(2) and 1.951(4) Å, respectively, whereas the

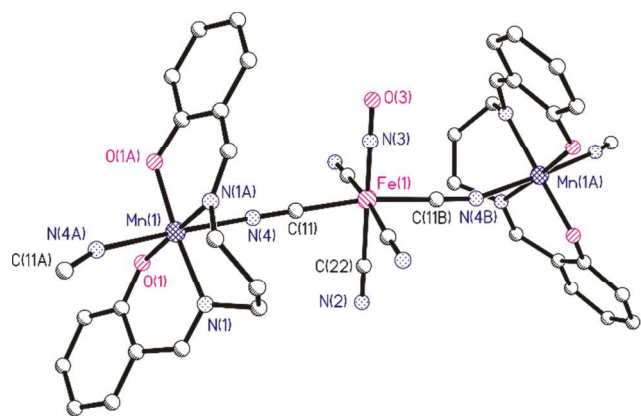


Fig. 1 The fragment of the 2D network in the structure of complex **1** showing the basic building unit and its connection mode.

Fe(1)–N(3) bond length is 1.664(3) Å (Table 2).

The structure of the  $[\text{Fe}(\text{CN})_5\text{NO}]^{2-}$  anion is in good agreement with the known nitroprusside complexes.<sup>17</sup> The  $[\text{Mn}(\text{salpn})]^+$  cations and  $[\text{Fe}(\text{CN})_5\text{NO}]^{2-}$  anions are linked to form a two dimensional (2D) neutral network via the cyanide bridges  $\text{Mn}^{\text{III}}-\text{N}=\text{C}-\text{Fe}^{\text{II}}$ , as shown in Fig. 2. In such a 2D network, each  $[\text{Mn}(\text{salpn})]^+$  cation is coordinated to two  $[\text{Fe}(\text{CN})_5\text{NO}]^{2-}$  anions via two CN groups in the axial positions, whereas each  $[\text{Fe}(\text{CN})_5\text{NO}]^{2-}$  anion is linked to four  $[\text{Mn}(\text{salpn})]^+$  cations through the four equatorial CN ligands,  $[\text{Fe}(\text{CN})(\mu\text{-CN})_4(\text{NO})\{\text{Mn}(\text{salpn})\}_2]_n$ . The intermetallic distance Fe(1)⋯Mn(1) is equal to 5.28(1) Å. The 2D networks in the structure of **1** are analogous to that in the structure of the complex  $\{[\text{Mn}(\text{salen})]_2[\text{Fe}(\text{CN})_5\text{NO}]\}_n$ .<sup>6b,c,d</sup>

Table 2 Selected bond lengths (Å) and bond angles (°) in **1**

Mn(1)–O(1)	1.891(1)	Mn(1)–N(1)	2.016(2)
Mn(1)–N(4)	2.288(2)	Fe(1)–N(3)	1.664(3)
Fe(1)–C(11)	1.935(2)	Fe(1)–C(22)	1.951(4)
O(1)–Mn(1)–O(1A)	93.0(1)	N(4A)–Mn(1)–N(4)	175.70(8)
O(1)–Mn(1)–N(1)	175.17(6)	N(3)–Fe(1)–C(11)	94.86(5)
O(1A)–Mn(1)–N(1)	90.21(7)	C(11)–Fe(1)–C(22)	85.14(5)
O(1)–Mn(1)–N(4)	94.56(6)	N(3)–Fe(1)–C(22)	180.0

Symmetry transformations used to generate equivalent atoms: A:  $-y+1, -x+1, -z+1/2$

Each NO ligand of the nitroprusside fragment in complex **1** is surrounded by four aromatic rings derived from four salpn ligands and one CN ligand from the adjacent layer (Fig. 3). The distance between O(3) atom and the centers of the aromatic rings is equal to 4.206 Å (4.228 Å in complex with salen), and the distance between O(3) and N(2) of the cyanide ligand is 3.165 Å (2.768 Å in complex with salen<sup>6b,c</sup>), which are slightly longer

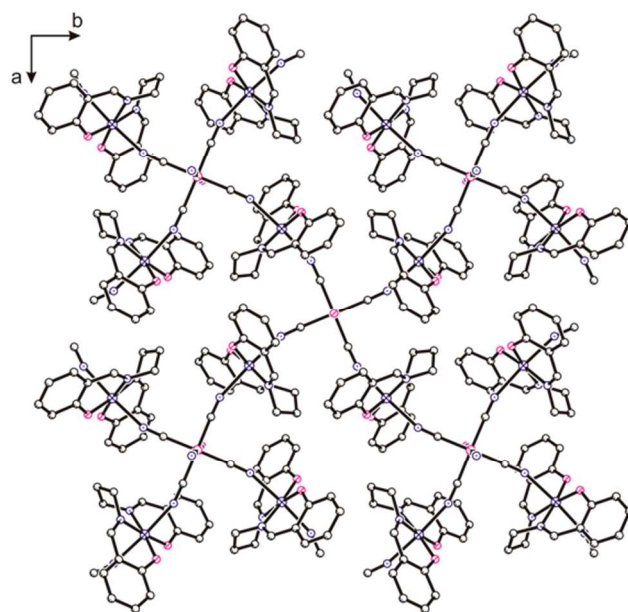


Fig. 2 The general view of the 2D layer in complex **1**.

than the sum of the van der Waals radii of O and N (3.15 Å). Thus, the aromatic rings are located practically identically relative to the NO group in the complexes with salen and salpn ligands, whereas the intermolecular contact O(3) with the nitrogen atom of the adjacent cyanide ligand is longer by ~0.4 Å in the salpn complex. In the 5-Brsalen complex, the NO group is surrounded by Br atoms from  $[\text{Mn}(5\text{-Brsalen})]^+$  cations from the adjacent layer with four short contacts  $\text{Br}\cdots\text{O}$  of 3.26 Å<sup>6a</sup> which are smaller than the sum of the van der Waals radii (3.37 Å). Thus, the NO group is less shielded in the structure of complex **1** as compared to analogous salen and 5-Brsalen bimetallic complexes.

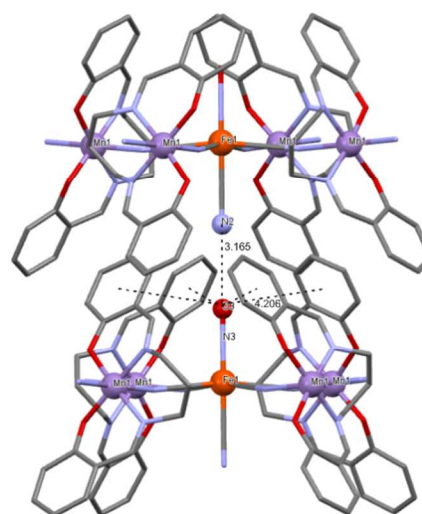


Fig. 3 The environment of the NO ligand in complex **1** (distances in Å).

Complex **2** crystallizes in the monoclinic  $C2/m$  space group and consists of isolated pentanuclear units  $\{[\text{Mn}^{\text{III}}(\text{salpn})(\text{CH}_3\text{OH})]_4[\text{Mn}^{\text{I}}(\text{CN})_5\text{NO}]\}^+$ , disordered tricyanomethanide anions  $[\text{C}(\text{CN})_3]^-$  and water molecules. In the pentanuclear complex cations four  $[\text{Mn}(\text{salpn})(\text{MeOH})]^+$  fragments are linked by the central  $[\text{Mn}(\text{CN})_5\text{NO}]^{3-}$  moiety through the four equatorial CN ligands,  $[\text{Mn}(\text{CN})(\mu\text{-CN})_4(\text{NO})\{\text{Mn}(\text{salpn})(\text{MeOH})\}_4]^+$  (Fig. 4).

Each  $\text{Mn}^{\text{III}}$  center is surrounded by two oxygen and two nitrogen atoms of the salpn ligand in the equatorial plane, one axial nitrogen atom of a cyanide bridge from the  $[\text{Mn}^{\text{I}}(\text{CN})_5\text{NO}]^{3-}$  unit and one axial oxygen atom from a terminal methanol molecule. In the equatorial plane of the  $\text{Mn}^{\text{III}}$  octahedra the average  $\text{Mn}^{\text{III}}\text{-X}$  bond length is 1.962(3) Å ( $\text{X}=\text{N}$  or  $\text{O}$  atom of the salpn ligand; Table 3). The Jahn–Teller distortion in the octahedral  $\text{Mn}^{\text{III}}$  ions leads to elongated axial  $\text{Mn}^{\text{III}}\text{-N}_{\text{cyanido}}$  and  $\text{Mn}^{\text{III}}\text{-O}_{\text{MeOH}}$  (2.232(5) and 2.342(4) Å) bonds.

The central  $[\text{Mn}^{\text{I}}(\text{CN})_5\text{NO}]^{3-}$  unit has a centrosymmetric structure which is in agreement with that of this anion in the complex  $\text{K}_3[\text{Mn}(\text{CN})_5\text{NO}]\cdot 2\text{H}_2\text{O}$ .<sup>18</sup> In **2**, the Mn(I) atom of  $[\text{Mn}^{\text{I}}(\text{CN})_5\text{NO}]^{3-}$  moiety occupies an inversion center giving rise to a disorder of the nitrosyl and terminal cyanide groups between two sites with 1/2 occupancies. The nitrosyl and terminal cyanide groups

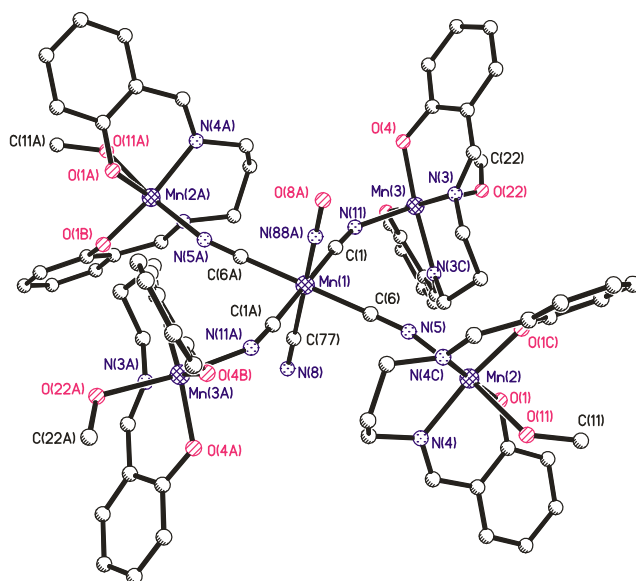


Fig. 4 General view of the  $[\text{Mn}(\text{CN})(\mu\text{-CN})_4(\text{NO})\{\text{Mn}(\text{salpn})(\text{MeOH})\}_4]$  cation. All H atoms, disordered NO and CN groups in the central  $[\text{Mn}(\text{CN})_5\text{NO}]^{3-}$  unit are omitted for clarity.

are disordered in two sites of 1/2 occupancies. The  $\text{Mn}^{\text{I}}\text{-C}$  bonds lengths are in the range of 1.964(8)–1.985(5) Å, whereas the  $\text{Mn}^{\text{I}}\text{-N}_{\text{NO}}$  bond length is 1.701(7) Å (Table 3). The  $\text{Mn}^{\text{I}}\text{-N-O}$  bond angle is linear. The average bond angles  $\text{Mn}^{\text{III}}\text{-N-C}$  and  $\text{N-C-Mn}^{\text{I}}$  are 159.0(4) and 177.7(5)°, respectively, and the average  $\text{Mn}^{\text{I}}\cdots\text{Mn}^{\text{III}}$  distance is *ca.* 5.27 Å.

As shown in Fig. S4, ESI†, the nearest surrounding of the NO group is formed by solvent water molecule O(3W) and aromatic rings from salpn fragments of the adjacent pentanuclear cation. The NO group is located at an  $\text{O}_{\text{NO}}\cdots\text{O}(3\text{W})$  distance of 3.131 Å and at an  $\text{O}_{\text{NO}}\cdots\text{C}$  distance of 3.292 Å, that are slightly larger than the sum of the van der Waals radii (3.04 and 3.22 Å, respectively). It should be noted that the occupancy of O(3W) water molecule sites is only 1/3 and hydrogen atoms in all solvent water molecules were not localized.

Table 3 Selected bond lengths (Å) and bond angles (°) in **2**

Mn(1)-C(77)	1.964(8)	Mn(1)-N(88)	1.701(7)
Mn(1)-C(1)	1.979(5)	Mn(1)-C(6)	1.985(5)
Mn(2)-O(1)*	1.896(3)	Mn(3)-O(4)*	1.889(3)
Mn(2)-O(1)	1.896(3)	Mn(3)-O(4)	1.889(3)
Mn(2)-N(4)*	2.030(3)	Mn(3)-N(3)*	2.031(3)
Mn(2)-N(4)	2.030(3)	Mn(3)-N(3)	2.031(3)
Mn(2)-N(5)	2.218(5)	Mn(3)-N(11)	2.245(5)
Mn(2)-O(11)	2.348(4)	Mn(3)-O(22)	2.335(4)
Mn(2)-N(5)-C(6)	162.2(4)	Mn(3)-N(11)-C(1)	155.8(4)
N(5)-C(6)-Mn(1)	178.5(5)	N(11)-C(1)-Mn(1)	176.9(5)

Symmetry transformations used to generate equivalent atoms: \* x, -y+1, z

Complex **3** crystallizes in the orthorhombic  $Pna2_1$  space group. The asymmetric unit includes two  $\{[\text{Mn}(\text{dapsc})][\text{Fe}(\text{CN})_5(\text{NO})]\}$  fragments in general positions, one methanol solvent and 1/2 of water molecule disordered on two sites of 1/3 and 1/6 occupancies. An ORTEP drawing of **3** is shown in Fig. 5, key bond distances and angles are listed in Table 4.

The crystal structure of **3** contains two independent neutral infinite chains  $\{[\text{Mn}(\text{dapsc})][\text{Fe}(\text{CN})_5(\text{NO})]\}_\infty$  running along the the crystallographic *c*-axis. They consist of alternating cationic  $[\text{Mn}^{\text{II}}(\text{dapsc})]^{2+}$  and anionic  $[\text{Fe}^{\text{II}}(\text{CN})_5(\text{NO})]^{2-}$  units connected through cyanide bridges,  $[\text{Fe}(\text{CN})_3(\mu\text{-CN})_2(\text{NO})\text{Mn}(\text{dapsc})]_\infty$  (Fig. 5). As far as we know, the complex **3** is the first structurally characterized nitroprusside-derived Mn(II)-Fe(II) 1D chain complex of the described  $[\text{Fe}(\text{CN})_5\text{NO}]\text{-Mn}(\text{II})(\text{ligand})$  compounds.<sup>19</sup> The Mn(II) ions are heptacoordinated by two oxygen and three nitrogen atoms of the dapsc ligand and two nitrogen atoms of cyanide bridges (pentagonal-bipyramidal geometry). Mn–O and Mn–N bond distances (Table 4) agree well with similar bonds in the published  $[\text{Mn}(\text{dapsc})\text{Cl}(\text{H}_2\text{O})]\text{Cl}\cdot 2\text{H}_2\text{O}$  complex.<sup>10e</sup>

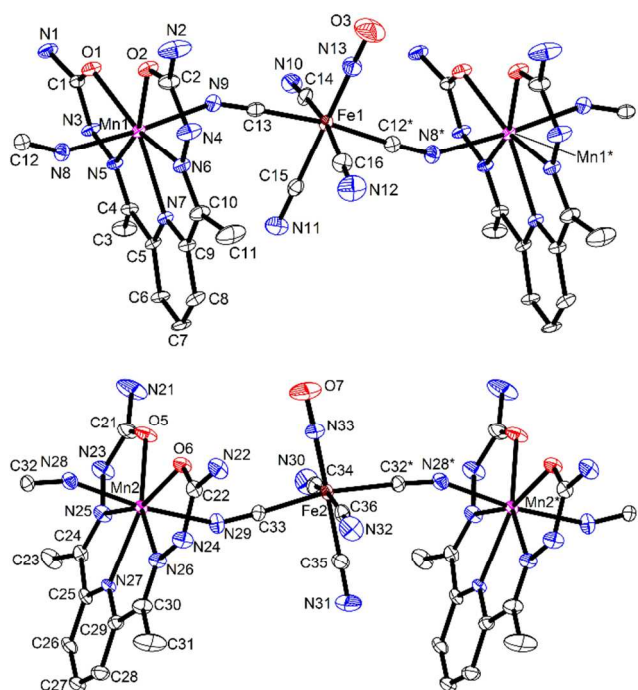


**Fig. 5** Fragments of two independent chains in **3** with atom numbering scheme (ORTEP drawing with 50% probability ellipsoids). Symmetry code: \* ( $x, y, z+1$ ).

The dapsac ligand is neutral since semicarbazone NH-groups are fully protonated and form strong hydrogen bonds to nitrogen atoms of NP from neighboring chains (corresponding N–H...N=C distances are 2.04, 2.21 Å for Mn(1)dapsac and 1.95, 1.98 Å for Mn(2)dapsac). The Mn(dapsac) fragments are quite flat. Maximal deviations from planarity within each of the semicarbazone arms (in the planes defined by 7 non-metallic atoms of two pentagonal cycles) are 0.039(3) Å for Mn(1)dapsac and 0.033(3) Å for Mn(2)dapsac. The dihedral angles between the two planes are 4.37(7) and 2.38(8)° for Mn(1) and Mn(2) units, respectively.

Two  $[\text{Fe}(\text{CN})_5(\text{NO})]^{2-}$  fragments are fully ordered. Their geometry is close to that in the complex **1** (Table 4). NO-groups

**Table 4** Selected bond lengths (Å) and angles (°) in **3**

Mn(1)–O(1)	2.300(2)	Mn(2)–O(5)	2.206(2)
Mn(1)–O(2)	2.247(2)	Mn(2)–O(6)	2.248(2)
Mn(1)–N(5)	2.295(2)	Mn(2)–N(25)	2.290(3)
Mn(1)–N(6)	2.302(3)	Mn(2)–N(26)	2.274(2)
Mn(1)–N(7)	2.335(2)	Mn(2)–N(27)	2.297(2)
Mn(1)–N(8)	2.210(3)	Mn(2)–N(28)	2.213(3)
Mn(1)–N(9)	2.198(3)	Mn(2)–N(29)	2.222(3)
Fe(1)–C <sub>CN</sub>	1.916(3)–1.936(3)	Fe(2)–C <sub>CN</sub>	1.920(4)–1.931(3)
Fe(1)–N(13)	1.670(3)	Fe(2)–N(33)	1.663(3)
O(1)–Mn(1)–O(2)	87.57(8)	O(5)–Mn(2)–O(6)	84.36(8)
O(1)–Mn(1)–N(5)	69.45(8)	O(5)–Mn(2)–N(25)	69.56(9)
O(2)–Mn(1)–N(6)	69.86(8)	O(6)–Mn(2)–N(26)	70.37(9)
N(5)–Mn(1)–N(7)	67.00(8)	N(25)–Mn(2)–N(27)	67.67(9)
N(6)–Mn(1)–N(7)	66.28(9)	N(26)–Mn(2)–N(27)	68.10(9)
N(8)–Mn(1)–N(9)	175.9(1)	N(28)–Mn(2)–N(29)	172.5(1)
Mn(1)–N(8)–C(12)	152.6(3)	Mn(2)–N(28)–C(32)	155.2(3)
Mn(1)–N(9)–C(13)	152.8(3)	Mn(2)–N(29)–C(33)	152.4(3)
Fe(1)–C(13)–N(9)	177.4(3)	Fe(2)–C(33)–N(29)	176.3(3)
Fe(1)–C(12*)–N(8*)	176.4(3)	Fe(2)–C(32*)–N(28*)	176.3(3)
C(13)–Fe(1)–C(12*)	172.0(1)	C(33)–Fe(2)–C(32*)	169.3(1)
C(14)–Fe(1)–C(16)	167.7(1)	C(34)–Fe(2)–C(36)	167.2(1)
C(15)–Fe(1)–N(13)	178.4(1)	C(35)–Fe(2)–N(33)	178.8(2)

Symmetry code: \* ( $x, y, z+1$ )

from the adjacent non-equivalent chains are located at  $\text{O}_{\text{NO}}\dots\text{O}_{\text{NO}}$  distance of 3.458(7) Å (Fig. 6) that is larger than the sum of the van der Waals radii of O atoms (3.04 Å). The nearest surrounding of NO groups is formed by solvent molecules. The NO-group connected to Fe(1) center has contacts with the methanol molecule (distances  $\text{O}_{\text{NO}}\dots\text{O}_{\text{MeOH}}$  and  $\text{N}_{\text{NO}}\dots\text{O}_{\text{MeOH}}$  are 2.860(6) and 2.920(6) Å, respectively). These are not hydrogen bonds since the H atom of the methanol OH group is directed to the oxygen atom of the dapsac ligand. The NO-group of the Fe(2) unit lies near disordered solvent water molecule ( $\text{O}_{\text{NO}}\dots\text{O}_{\text{water}}$  distances are 2.72(3) and 2.78(2) Å, H atoms in water were not localized). Note that total occupancy of two

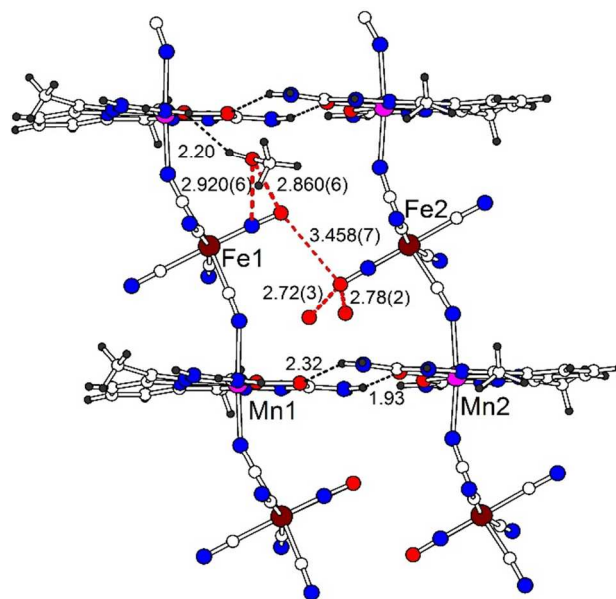




Fig. 6 Environment of the NO ligand in complex **3** (distances in Å).

disordered water sites is only 0.5. Other intermolecular distances from NO groups are longer than 3.5 Å.

Intrachain Mn–Fe distances are 5.1206(8), 5.1272(8) in the Mn(1)–Fe(1) chain and 5.1197(8), 5.1473(8) Å in the Mn(2)–Fe(2) chain. Mn–N–C angles are 152–155°. There is an extensive net of hydrogen bonds (N–H...O<sub>dapsc</sub>, NH<sub>2</sub>...N≡C) between the chains, some of them are shown in Fig. 6 by black dashed lines.

### Magnetic properties of **1** and **3**

The temperature dependencies of the magnetic susceptibility were measured on polycrystalline samples of **1** and **3** in the temperature range 2.0 K–300 K under the applied magnetic field of 0.1 T. The product  $\chi_M T(T)$  is depicted in Fig. 7. The room-temperature  $\chi_M T$  values are in good agreement with the paramagnetic response of the two magnetically non-interacting Mn(III) ions with  $S = 2$  ( $\chi_M T = 6.0 \text{ cm}^3 \text{ K/mol}$  for  $g = 2$ ) and one Mn(II) ion with  $S = 5/2$  ( $\chi_M T = 4.38 \text{ cm}^3 \text{ K/mol}$ ,  $g = 2$ ) for **1** and **3**, respectively. Hence, the Fe(II) cation does not contribute to the magnetic susceptibility, *i.e.* it has a low spin electronic configuration with  $S = 0$ . The  $\chi_M T$  value for **1** remains nearly constant upon cooling down to 30 K and decreases sharply at lower temperatures (Fig. 7). This decrease is most likely due to zero-field splitting (ZFS) of anisotropic high-spin Mn<sup>3+</sup> ions.

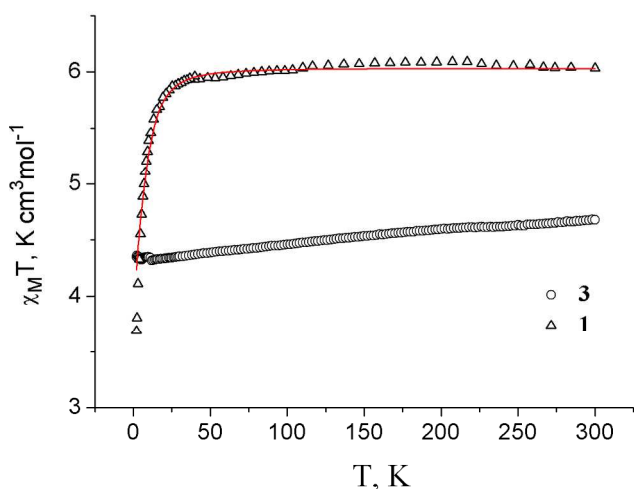


Fig. 7 Plot of the  $\chi_M T$  product vs  $T$  for complexes **1**, **3**. Solid red line shows the best obtained fit for **1**.

The observed temperature behavior of  $\chi_M T$  is typical for weakly antiferromagnetically interacting spin carriers, namely, [Mn(III)(SB)]<sup>+</sup> units via diamagnetic [N≡C–(Fe(CN)<sub>3</sub>NO)–C≡N] linkers.<sup>6a,b,c</sup> The  $\chi_M T$  product vs  $T$  for **1** was fitted (Fig. 7, solid red line) taking into account only ZFS of Mn<sup>3+</sup> by using the *PHI* program.<sup>20</sup> The best-fit parameters of the magnetic data are  $D = -6.5 \text{ cm}^{-1}$ ,  $g = 2.01$ . The obtained value of  $D$  is almost two times higher than the characteristic value for Mn<sup>3+</sup> ions suggesting that a weak antiferromagnetic exchange through the diamagnetic

nitroprusside anions should also be taken into account. However, the estimation of exchange coupling constants in 2D magnetic lattice cannot be carried out due to the complexity of the problem. This problem was discussed previously for similar 2D compounds  $\{[\text{Mn}(5\text{-Brsalen})]_2[\text{Fe}(\text{CN})_5(\text{NO})]\}_n$  and  $\{[\text{Mn}(\text{salen})]_2[\text{Fe}(\text{CN})_5(\text{NO})] \cdot 2\text{H}_2\text{O}\}_n$ <sup>6a,b</sup>.

In the case of complex Mn<sup>2+</sup> (**3**), the  $\chi_M T$  product decreases slightly on lowering the temperature down to 2 K (Fig. 7). In contrast to the complexes Mn<sup>3+</sup>, ZFS for the Mn<sup>2+</sup> ions is negligible and does not noticeably influence the low-temperature pattern of  $\chi_M T$ .<sup>21</sup> The  $\chi_M^{-1}(T)$  vs  $T$  for **3** follows fairly well the Curie-Weiss law over the entire temperature range with a Curie constant ( $C$ ) of  $4.67 \text{ cm}^3 \text{ K/mol}$  and a negative Weiss constant ( $\theta$ ) of  $-2.75 \text{ K}$ , meaning that minimal antiferromagnetic interactions are operative between [Mn(dapsc)] cations in the infinite chains through the diamagnetic nitroprusside anion bridges.

### Photochromic properties of **1** and **3**

Two important informations can be obtained from infrared spectroscopy. One is related to the structure of the heterometallic chain complexes and the other to the light-induced metastable linkage NO-isomers after irradiation with light. In both samples **1** and **3** light-induced metastable linkage isomers could be generated by irradiation in the spectral range of 400 – 500 nm. In sample **1** a population of 3% of MS1 and MS2 can be obtained and we present in Fig. 8 the corresponding increase of the new  $\nu(\text{NO})$  vibrational absorption bands at  $1793 \text{ cm}^{-1}$  (MS1) for different irradiation wavelengths of 476 nm, 445 nm and 405 nm (maximum) and the increase of the new  $\nu(\text{NO})$  band at  $1654 \text{ cm}^{-1}$  (MS2).

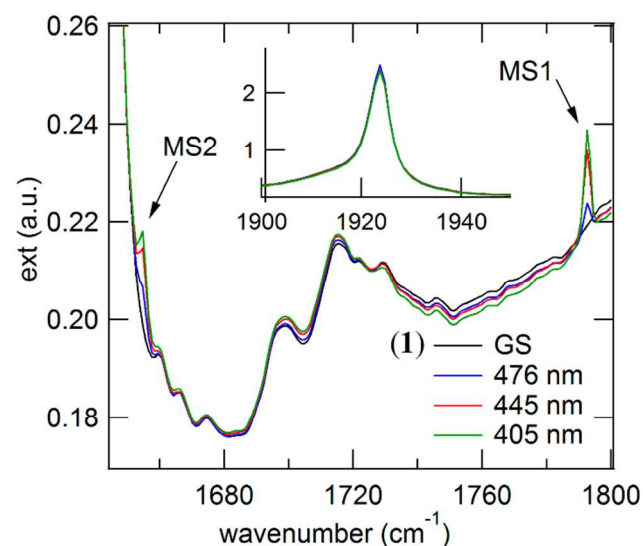


Fig. 8 Increase of the population for the irradiation wavelengths 476 nm, 445 nm, 405 nm of  $\nu(\text{NO})$  MS1 and  $\nu(\text{NO})$  MS2. The insert shows the  $\nu(\text{NO})$  vibration of GS.

The ground state  $\nu(\text{NO})$  vibrational band at  $1924\text{ cm}^{-1}$  decreases by 3% and the energy shifts of the linkage isomers are  $123\text{ cm}^{-1}$  for MS1 and  $270\text{ cm}^{-1}$  for MS2 to lower wavenumbers. There is only one strong  $\nu(\text{NO})$  vibration of GS (insert in Fig. 8) and due to  $4m$  symmetry only 4  $\nu(\text{CN})$  stretching vibrations in GS at  $2179\text{ cm}^{-1}$ ,  $2170\text{ cm}^{-1}$ ,  $2163\text{ cm}^{-1}$ ,  $2151\text{ cm}^{-1}$ . No splittings could be observed with a resolution of  $2\text{ cm}^{-1}$  at 10 K. This is a clear indication of a perfectly ordered structural incorporation of the  $[\text{Fe}(\text{CN})_5\text{NO}]^{2-}$  anion via bondings between  $\text{Mn}(1)\text{-N}(4)\text{-C}(11)$  and  $\text{Mn}(1\text{A})\text{-N}(4\text{B})\text{-C}(11\text{B})$  as presented in Fig. 1 without any distortion of the nitroprusside anion by surrounding atoms. Furthermore, the first overtone  $2\nu(\text{NO})$  at  $3823\text{ cm}^{-1}$  is again a single band and the anharmonicity is  $25\text{ cm}^{-1}$  which is a normal value for all nitroprussides.<sup>22</sup> The free space around the NO ligand is large enough for free NO rotation going from  $\text{Fe-N-O}$  to  $\text{Fe-O-N}$ . In sample **3** the population of MS1 is higher with 8% and the structure of two independent chains as presented in Fig. 5 is clearly reflected in the splitting of the  $\nu(\text{CN})$  and  $\nu(\text{NO})$  stretching vibrations. As shown in Fig. 9 in the spectral range of  $2250 - 1750\text{ cm}^{-1}$  there are at least 8  $\nu(\text{CN})$  vibrations divided in two groups of four vibrations, 4  $\nu(\text{NO})$  vibrations again divided into two groups at  $1903\text{ cm}^{-1}$ ,  $1912\text{ cm}^{-1}$  (shoulder),  $1921\text{ cm}^{-1}$  and  $1926\text{ cm}^{-1}$  (shoulder) and two new  $\nu(\text{NO})$  vibrations of MS1 at  $1785\text{ cm}^{-1}$  and  $1793\text{ cm}^{-1}$ .

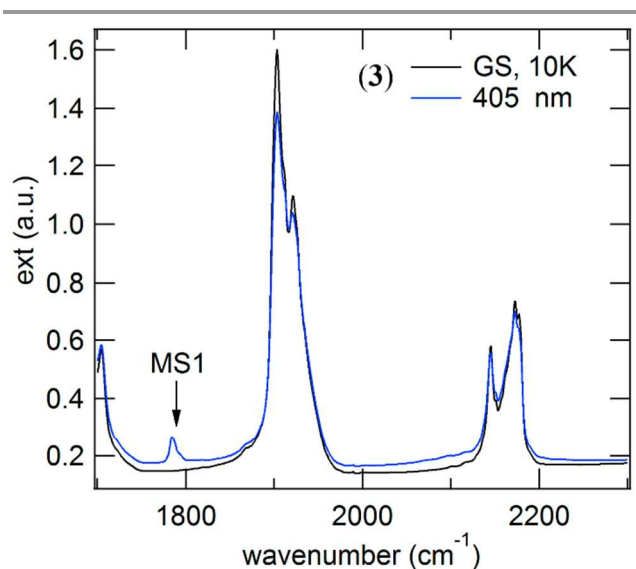


Fig. 9 Vibrational bands of  $\nu(\text{CN})$ ,  $\nu(\text{NO})$  and the down shifted  $\nu(\text{NO})$  vibration of MS1.

The maximum population of 8 % for MS1 can be reached by irradiation with 405 nm. Due to the strong absorption band starting at  $1700\text{ cm}^{-1}$  MS2 cannot be observed as a separate vibrational  $\nu(\text{NO})$  band. However, irradiation with 1064 nm with which MS1 is transferred into MS2 shows that the  $\nu(\text{NO})$  band of MS1 disappears completely but the  $\nu(\text{NO})$  band of GS has not reached its original (non-irradiated) GS-area. Consequently, MS2 can be populated but not directly observed by IR spectroscopy. The two-chain structure can be precisely

seen in the first overtones of the  $\nu(\text{NO})$  vibrations. There are two groups with two bands:  $3821\text{ cm}^{-1}$ ,  $3815\text{ cm}^{-1}$  and  $3792\text{ cm}^{-1}$ ,  $3787\text{ cm}^{-1}$ . These four clearly resolved bands indicate either a variation in the bonds inside the chains or a distortion by surrounding atoms in the near of the NO ligand. Due to the splitting of the  $\nu(\text{CN})$  vibrations into two groups of four vibrations and due to the two independent chains, we assume an influence by the surrounding atoms of the NO ligands.

## Conclusions

In this report, four new compounds derived from photochromic  $[\text{Fe}(\text{CN})_5\text{NO}]^{2-}$ , its isoelectronic analog  $[\text{Mn}(\text{CN})_5\text{NO}]^{3-}$ , paramagnetic  $[\text{Mn}^{3+}(\text{salpn})]^+$  and  $[\text{Mn}^{2+}(\text{dapsc})]^{2+}$  building blocks have been obtained:  $\{[\text{Mn}(\text{salpn})]_2[\text{Fe}(\text{CN})_5(\text{NO})]\}_n$  (**1**),  $\{[\text{Mn}(\text{salpn})(\text{CH}_3\text{OH})]_4[\text{Mn}(\text{CN})_5\text{NO}]\}[\text{C}(\text{CN})_3]\cdot 3\text{H}_2\text{O}$  (**2**),  $\{[\text{Mn}(\text{dapsc})][\text{Fe}(\text{CN})_5\text{NO}]\cdot 0.5\text{CH}_3\text{OH}\cdot 0.25\text{H}_2\text{O}\}_n$  (**3**),  $\{[\text{Mn}(\text{salpn})(\text{CH}_3\text{OH})]_4[\text{Fe}(\text{CN})_5\text{NO}]\}(\text{ClO}_4)_2\cdot 4\text{H}_2\text{O}$  (**4**). The single crystal X-ray analysis shows that **1** possesses an extended 2D neutral network, **3** has a chain structure and **2**, **4** represent discrete pentanuclear complexes. The structural differences in the samples **1** and **3** are confirmed by IR-spectroscopy due to the  $\nu(\text{NO})$  and  $\nu(\text{CN})$  band splitting in  $[\text{Fe}(\text{CN})_5\text{NO}]^{2-}$ . The spatial arrangement of the ordered NO group in the structures of **1**, **3** has been analyzed in detail and established the availability of some free space required for isomerizing the NO group under exposure to light. The paramagnetism given by the Mn complexes (**1**, **3**) and the coordination of cyanido groups with  $\text{Mn}^{\text{III}}$  or  $\text{Mn}^{\text{II}}$  ions do not inhibit the presence and production of light-induced linkage isomers. The decay temperature of the linkage isomers is at about 140 K, which is comparable to other known  $[\text{Fe}(\text{CN})_5\text{NO}]^{2-}$  compounds.<sup>23</sup> The population of metastable states is low (3% and 8% in **1** and **3**, respectively) that is explained by the overlap of the absorption bands in the visible spectral range between GS and the metastable states as discussed for  $\text{Na}_2[\text{Fe}(\text{CN})_5\text{NO}]\cdot 2\text{H}_2\text{O}$ .<sup>24</sup> If the absorption bands of GS and MS have a strong overlap it is possible to populate and depopulate with one and the same wavelength so that an equilibrium occurs between the occupation of MS and the back process out of MS. This behavior depends on the position of the energy bands of GS with respect to MS.

## Acknowledgements

This work was supported by the Russian Foundation for Basic Research, project No. 13-03-12418.

## Notes and references

<sup>a</sup> Institute of Problems of Chemical Physics, Chernogolovka, Moscow District, 1 Academician Semenov av., 142432 Russian Federation. E-mail: yagubski@icp.ac.ru, slavaoven@mail.ru; Fax: +7 496-5225636; Tel: +7 495-9935707

<sup>b</sup> Institute of Solid State Physics, Chernogolovka, Moscow District, 2 Academician Ossipyan str., 142432 Russian Federation. E-mail: zorina@issp.ac.ru;

Fax: +7 496-5228160; Tel: +7 496-5221982

<sup>c</sup> Université de Lorraine, CRM2, UMR 7036, Vandoeuvre-les-Nancy, F-54506, France. E-mail: dominik.schaniel@univ-lorraine.fr;

Fax: +33 (0) 383 68 4300; Tel: +33 (0) 383 68 4863

<sup>d</sup> CNRS, CRM<sup>2</sup>, UMR 7036, Vandoeuvre-les-Nancy, F-54506, France. E-mail: dominik.schaniel@univ-lorraine.fr;

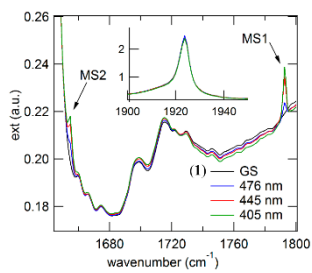
<sup>e</sup> Technische Universität Dresden, Institut für Strukturphysik, Zellescher Weg 16, 01069 Dresden, Germany. E-mail: theo.woike@tu-dresden.de

Fax: +49 351 463-37048; Tel: +49 351 463-34670

† Electronic Supplementary Information (ESI) available: Fig. S1-S4. The TG, DSC and MS curves for complexes (1) and (3), Figures S1, S2. The general view of the structure of complex (4), Figure S3. The environment of NO ligand in complex (2), Figure S4. X-ray crystallographic files, in CIF format, for complexes (1), (2) and (3). The X-ray crystal structure data have been deposited with the Cambridge Crystallographic Data Center, with reference codes CCDC 1022451, 1022452, and 1022887. For ESI and crystallographic data in CIF or other electronic format see DOI: 10.1039/b000000x/

- (a) F. M. Ashmawy, C. A. McAuliffe, R. V. (Dick) Parish and J. Tames, *J. Chem. Soc. Dalton Trans.*, 1985, 1391; (b) A. R. Oki and D. Hodgson, *J. Inorg. Chim. Acta.*, 1990, **170**, 65; (c) H. Miyasaka, N. Matsumoto, H. Okawa, N. Re, E. Gallo and C. Floriani, *Angew. Chem., Int. Ed. Eng.*, 1995, **34**, 1446; (d) N. Re, E. Gallo, C. Floriani, H. Miyasaka and N. Matsumoto, *Inorg. Chem.*, 1996, **35**, 6004; (e) F. Sakamoto, T. Sumiya, M. Fujita, T. Tada, X.-S. Tan, E. Suzuki, I. Okura and Y. Fujii, *Chem. Lett.*, 1998, **27**, 1127; (f) H. Miyasaka, R. Clérac, T. Ishii, H.-C. Chang, S. Kitagawa and M. Yamashita, *J. Chem. Soc. Dalton Trans.*, 2002, 1528; (g) L. Lecren, W. Wernsdorfer, Y.-G. Li, A. Vindigni, H. Miyasaka and R. Clérac, *J. Am. Chem. Soc.*, 2007, **129**, 5045; (h) P. Kar, P. M. Guha, M. G. B. D. Drew, T. Ishida and A. Ghosh, *Eur. J. Inorg. Chem.*, 2011, 2075; (i) P. Kar, R. Biswas, M. G. B. Drew, Y. Ida, T. Ishida and A. Ghosh, *Dalton Trans.*, 2011, **40**, 3295.
- (a) H. Miyasaka, N. Matsumoto, H. Okawa, N. Re, E. Gallo and C. Floriani, *J. Am. Chem. Soc.*, 1996, **118**, 981; (b) H. Miyasaka, R. Clérac, W. Wernsdorfer, L. Lecren, C. Bonhomme, K.-I. Sugiura and M. Yamashita, *Angew. Chem., Int. Ed. Eng.*, 2004, **43**, 2801; (c) Z. Lu, M. Yuan, F. Pan, S. Gao, D. Zhang and D. Zhu, *Inorg. Chem.*, 2006, **45**, 3538; (d) H. J. Choi, J. J. Sokol and J. R. Long, *Inorg. Chem.*, 2004, **43**, 1606; (e) H. Miyasaka, H. Ieda, N. Matsumoto, N. Re, R. Crescenzi and R. Floriani, *Inorg. Chem.*, 1998, **37**, 255; (f) H. H. Ko, J. H. Lim, H. S. Yoo, J. S. Kang, H. C. Kim, E. K. Koh and C. S. Hong, *Dalton Trans.*, 2007, 2070; (g) P. Przychodzen, M. Rams, C. Guyard-Duhayon and B. Sieklucka, *Inorg. Chem. Commun.*, 2005, **8**, 350; (h) M. Ferbinteanu, H. Miyasaka, W. Wernsdorfer, K. Nakata, K. Sugiura, M. Yamashita, C. Coulon and R. Clérac, *J. Am. Chem. Soc.*, 2005, **127**, 3090; (i) H. S. Yoo, H. H. Ko, D. W. Ryo, J. W. Lee, J. H. Yoon, W. R. Lee, H. C. Kim, E. K. Kon and C. S. Hong, *Inorg. Chem.*, 2009, **48**, 5617; (j) H. Miyasaka, H. Okawa, A. Miyazaki and T. Enoki, *Inorg. Chem.*, 1998, **37**, 4878; (k) H. Z. Kou, Z. H. Ni, B. C. Zhou and R. J. Wang, *Inorg. Chem. Commun.*, 2004, **7**, 1150; (l) H.-B. Zhou, J. Wang, H.-S. Wang, Y.-L. Xu, X.-J. Song, Y. Song and X.-Z. You, *Inorg. Chem.*, 2011, **50**, 6868; (m) J. Dreiser, K. S. Pedersen, A. Schnegg, K. Holldack, J. Nehrkorn, M. Sigrist, P. Tregenna-Piggott, H. Mutka, H. Weihe, V. S. Mironov, J. Bendix and O. Waldmann, *Chem. Eur. J.*, 2013, **19**, 3693; (n) H. Miyasaka, A. Saitoh and S. Abe, *Coord. Chem. Rev.*, 2007, **251**, 2622 and references therein; (o) H. Miyasaka, T. Madanbashi, A. Saitoh, N. Motokawa, R. Ishikawa, M. Yamashita, S. Bahr, W. Wernsdorfer and R. Clérac, *Chem. Eur. J.* 2012, **18**, 3942.
- (a) C. Kachi-Terajima, H. Miyasaka, K. Sugiura, R. Clérac and H. Nojiri, *Inorg. Chem.*, 2006, **45**, 4381; (b) K. S. Pedersen, J. Bendix and R. Clérac, *Chem. Commun.*, 2014, **50**, 4396.
- (a) H. Miyasaka and R. Clérac, *Bull. Chem. Soc. Jpn.*, 2005, **78**, 1725; (b) R. Clérac, H. Miyasaka, M. Yamashita and C. Coulon, *J. Am. Chem. Soc.*, 2002, **124**, 12837; (c) H. Miyasaka, T. Madanbashi, K. Sugimoto, Y. Nakazawa, W. Wernsdorfer, K. Sugiura, M. Yamashita, C. Coulon and R. Clérac, *Chem. Eur. J.*, 2006, **12**, 7028; (d) H. Sun, Z. Wang and S. Gao, *Coord. Chem. Rev.*, 2010, **254**, 1081; (e) W.-X. Zhang, R. Ishikawa, B. Breedlove and M. Yamashita, *RSC Advances*, 2013, **3**, 3772.
- (a) Z.-H. Ni, L. Zheng, L.-F. Zhang, A.-L. Cui, W.-W. Ni, C.-C. Zhao and H.-Z. Kou, *Eur. J. Inorg. Chem.*, 2007, **2007**, 1240; (b) H.-B. Zhou, Z.-C. Zhang, Y. Chen, Y. Song and X.-Z. You, *Polyhedron* 2011, **30**, 3158.
- (a) M. Clemente-Leon, E. Coronado, J. R. Galan-Mascaros, C. J. Gomez-Garcia, Th. Woike and J. M. Clemente-Juan, *Inorg. Chem.*, 2001, **40**, 87; (b) R. Ababei, Y.-G. Li, O. Roubeau, M. Kalisz, N. Brefuel, C. Coulon, E. Harte, X. Liu, C. Mathonière and R. Clérac, *New. J. Chem.*, 2009, **33**, 1237; (c) C. Yang, Q.-L. Wang, Y. Ma, G.-T. Tang, D.-Z. Liao, S.-P. Yan, G.-M. Yang and P. Cheng, *Inorg. Chem.*, 2010, **49**, 2047; (d) H.-Q. Shu, Y. Xu and X.-P. Shen, *J. Chem. Crystallogr.*, 2011, **41**, 1218.
- (a) P. Gutlich, Y. Garcia and Th. Woike, *Coord. Chem. Rev.*, 2001, **219–221**, 839 and references therein; (b) M. D. Carducci, M. R. Pressprich and P. Coppens, *J. Amer. Chem. Soc.*, 1997, **119**, 2669; (c) P. Coppens, I. Novozhilova and A. Kovalevsky, *Chem. Rev.*, 2002, **102**, 861; (d) D. Schaniel, Th. Woike, J. Schefer and V. Petricek, *Phys. Rev. B*, 2005, **71**, 174112; (e) L. E. Hatcher and P. R. Raithby, *Acta Cryst. C*, 2013, **69**, 1448.
- (a) S. Benard, E. Riviere, P. Yu, K. Nakatani and J. F. Delouis, *Chem. Mater.*, 2001, **13**, 159; (b) M. Okubo, M. Enomoto and N. Kojima, *Solid State Commun.*, 2005, **134**, 777; (c) I. Kashima, M. Okubo, Y. Qno, N. Kida, M. Hikita, M. Enomoto and N. Kojima,

- Synth. Met.*, 2005, **155**, 703; (d) L. A. Kushch, L. S. Kurochkina, E. B. Yagubskii, G. V. Shilov, S. M. Aldoshin, V. A. Emel'yanov, Yu. N. Shvachko, V. S. Mironov, D. Schaniel, Th. Woike, C. Carbonera and C. Mathoniere, *Eur. J. Inorg. Chem.*, 2006, **2006**, 4074; (e) L. A. Kushch, E. B. Yagubskii, M. Il'in, D. Schaniel, Th. Woike, S. Golhen, O. Cadore and L. J. Ouahab, *Cluster. Sci.*, 2006, **17**, 303; (f) D. Schaniel, Th. Woike, L. Kushch and E. Yagubskii, *Chem. Phys.*, 2007, **340**, 211; (g) S. M. Aldoshin, *J. Photochem. Photobiol. A: Chem.*, 2008, **200**, 19; (h) E. B. Yagubski and L. A. Kushch, *Nanotech. in Russia*, 2008, **3**, 151; (i) L. A. Kushch, E. B. Yagubskii, A. I. Dmitriev, R. B. Morgunov, V. A. Emel'yanov, A. R. Mustafina, A. T. Gubaidullin, V. A. Burirov, S. E. Solovieva, D. Schaniel and Th. Woike, *Physica B*, 2010, **405**, S30.
- 9 (a) L. A. Kushch, V. D. Sasnovskaya, E. B. Yagubskii, S. S. Khasanov, S. V. Simonov, R. P. Shibaeva, A. V. Korolev, D. V. Starichenko, A. O. Anokhin, V. Yu. Irkhin and Yu. N. Shvachko, *Inorg. Chim. Acta*, 2011, **378**, 169; (b) E. V. Peresypkina and K. E. Vostrikova, *Dalton Trans.*, 2012, **41**, 4100.
- 10 (a) D. W. Wester and G. J. Palenik, *J. Amer. Chem. Soc.*, 1973, **95**, 6505; (b) D. W. Wester and G. J. Palenik, *J. Amer. Chem. Soc.*, 1974, **96**, 7565; (c) G. J. Palenik, *Inorg. Chem.*, 1976, **15**, 755; (d) G. J. Palenik, D. W. Wester, U. Rychlewska and R. C. Palenik, *Inorg. Chem.*, 1976, **15**, 1814; (e) G. J. Palenik and D. W. Wester, *Inorg. Chem.*, 1978, **17**, 864; (f) A. Bino, R. Frim and M. Van Genderen, *Inorg. Chim. Acta*, 1987, **127**, 95; (g) M. Carcelli, S. Ianelli, P. Pelagatti and G. Pelizzi, *Inorg. Chim. Acta*, 1999, **292**, 121; (h) M. Gerloch, I. Morgenstern-Badarau and J.- P. Audiere, *Inorg. Chem.*, 1979, **18**, 3220; (i) M. Gerloch and I. Morgenstern-Badarau, *Inorg. Chem.*, 1979, **18**, 3225; (j) P. Kaur, W. T. Robinson and K. Singh, *J. Coord. Chem.*, 2002, **55**, 281; (k) P. Kaur, A. Sarangal, E. McInnes and W. T. Robinson, *J. Coord. Chem.*, 2004, **57**, 797.
- 11 R. Ruamps, L. J. Batchelor, R. Maurice, N. Gogoi, P. Jimenez-Lozano, N. Guihery, C. de Graaf, A.- L. Barra, J.- P. Sutter and T. Mallah, *Chem. Eur. J.*, 2013, **19**, 950.
- 12 V. A. Kopotkov, S. V. Simonov, O. V. Koplak, A. I. Dmitriev and E. B. Yagubskii, *Russ. Chem. Bull., Int. Ed.*, 2013, **62**, 1777.
- 13 F. A. Cotton, R. R. Monchamp, R. J. M. Henry and R. C. Young, *J. Inorg. Nucl. Chem.*, 1959, **10**, 28.
- 14 Agilent, CrysAlis PRO, version 171.35.19, Agilent Technologies Ltd, Yarnton, Oxfordshire, England, 2011.
- 15 G.M. Sheldrick, SHELXTL, version 6.14, Structure Determination Software Suite, Bruker AXS, Madison, Wisconsin, USA 2000.
- 16 G. M. Sheldrick, *Acta Cryst., Sect. A*, 2008, **64**, 112.
- 17 (a) H. L. Shyu, H. H. Wie and Y. Wang, *Inorg. Chim. Acta*, 1997, **258**, 81; (b) Z. N. Chen, J. L. Wang, J. Qiu, F. G. Miao and W. X. Tang, *Inorg. Chem.*, 1995, **34**, 2255.
- 18 A. Tullberg and N.- G. Vannerberg, *Acta Chem. Scand.*, 1967, **21**, 1462.
- 19 (a) W.-W. Ni, H.-Z. Kou, Z.-H. Ni and R.-J. Wang, *J. Chem. Crystallogr.*, 2006, **36**, 48; (b) S.-W. Liang, M.-X. Li, M. Shao and H.-J. Liu, *J. Mol. Struct.*, 2007, **841**, 73.
- 20 N. F. Chilton, R. P. Anderson, L. D. Turner, A. Soncini and K. S. Murray, *J. Comput. Chem.* 2013, **34**, 1164.
- 21 L. A. Kushch, E. B. Yagubskii, S. V. Simonov, R. P. Shibaeva, E. A. Sutura, N. P. Gritsan, A. V. Sadakov and I. V. Sulimenkov, *Eur. J. Inorg. Chem.*, 2013, **2013**, 5603 and references therein.
- 22 M. E. Chacon Villalba, J. A. Güida, E. L. Varetti and P. J. Aymonino, *J. Spectrochim. Acta A*, 2001, **57**, 367.
- 23 H. Zöllner, W. Kraser, Th. Woike and S. Hausstühl, *Chem. Phys. Lett.*, 1989, **161**, 497.
- 24 D. Schaniel, J. Schefer, B. Delley, M. Imlau and Th. Woike, *Phys. Rev. B*, 2002, **66**, 085103.



The cyano-bridged 1- and 2-D complexes built from photochromic  $[\text{Fe}(\text{CN})_5\text{NO}]^{2-}$  and paramagnetic  $[\text{Mn}^{\text{II}}(\text{dapsc})]^{2+}$  and  $[\text{Mn}^{\text{III}}(\text{salpn})]^+$  building blocks have been obtained and exhibited photochromic properties induced by the presence of the nitroprusside anion.